Structural Basis for Interactions Between Contactin Family Members and Protein Tyrosine Phosphatase Receptor Type G in Neural Tissues

Roman M. Nikolaienko, Michal Hammel, Véronique Dubreuil, Rana Zalmai, David R. Hall, Nurjahan Mehzabeen, Sebastian J. Karuppan, Sheila Harroch, Salvatore L. Stella and Samuel Bouyain

SUPPLEMENTARY TABLES AND FIGURES

Table S1. Curve-fitting parameters obtained for each AlphaScreen bead-based competition assay.

Inhibitor	Immobilized proteins	IC_{50} (nM)	R^2	Signal/Noise	Points analyzed	Outliers	95% confidence interval
PTPRZ(CA)	PTPRZ(CA) CNTN1-Fc	353	0.99	1051	20	0	283 to 441 nM
PTPRZ(CA)	PTPRZ(CA) CNTN1-Fc	316	0.99	1307	19	0	242 to 413 nM
PTPRZ(CA)	PTPRZ(CA) CNTN1-Fc	328	0.98	417	19	0	224 to 481 nM
PTPRZ(CA)	PTPRZ(CA) CNTN1-Fc	332	0.93	445	17	2	157 to 705 nM
PTPRG(CA)	PTPRG(CA) CNTN3-Fc	306	0.98	994	18	1	224 to 418 nM
PTPRG(CA)	PTPRG(CA) CNTN3-Fc	437	0.98	997	19	0	324 to 589 nM
PTPRG(CA)	PTPRG(CA) CNTN3-Fc	465	0.99	1019	19	0	372 to 580 nM
PTPRG(CA)	PTPRG(CA) CNTN3-Fc	418	0.99	1206	18	1	365 to 479 nM
PTPRG(CA)	PTPRG(CA) CNTN3-Fc	564	0.98	932	19	0	408 to 780 nM
PTPRG(CA)	PTPRG(CA) CNTN3-Fc	412	0.99	780	19	0	315 to 538 nM
PTPRG(CA)	PTPRG(CA) CNTN3-Fc	397	0.98	621	19	0	282 to 559 nM
PTPRG(CA)	PTPRG(CA) CNTN4-Fc	146	0.98	303	19	0	103 to 205 nM
PTPRG(CA)	PTPRG(CA) CNTN4-Fc	192	0.98	364	19	0	142 to 259 nM
PTPRG(CA)	PTPRG(CA) CNTN4-Fc	207	0.99	605	19	0	173 to 248 nM
PTPRG(CA)	PTPRG(CA) CNTN4-Fc	235	0.99	579	19	0	193 to 287 nM
PTPRG(CA)	PTPRG(CA) CNTN4-Fc	153	0.96	303	19	0	92 to 254 nM
PTPRG(CA)	PTPRG(CA) CNTN4-Fc	236	0.99	729	17	2	202 to 274 nM
PTPRG(CA)	PTPRG(CA) CNTN4-Fc	297	0.99	460	19	0	239 to 367 nM
PTPRG(CA)	PTPRG(CA) CNTN4-Fc	343	0.98	183	19	0	261 to 451 nM
PTPRG(CA)	PTPRG(CA) CNTN4-Fc	236	0.97	350	19	0	187 to 296 nM
PTPRG(CA)	PTPRG(CA) CNTN4-Fc	305	0.98	193	19	0	230 to 401 nM
PTPRG(CA)	PTPRG(CA) CNTN5-Fc	311	0.99	802	19	0	257 to 377 nM

PTPRG(CA)	PTPRG(CA) CNTN5-Fc	298	0.99	1511	19	0	245 to 362 nM
PTPRG(CA)	PTPRG(CA) CNTN5-Fc	395	0.98	1334	18	1	288 to 541 nM
PTPRG(CA)	PTPRG(CA) CNTN5-Fc	315	0.99	678	19	0	243 to 409 nM
PTPRG(CA)	PTPRG(CA) CNTN5-Fc	317	0.98	606	18	1	236 to 426 nM
PTPRG(CA)	PTPRG(CA) CNTN6-Fc	397	0.98	289	19	0	287 to 550 nM
PTPRG(CA)	PTPRG(CA) CNTN6-Fc	636	0.99	431	17	2	490 to 824 nM
PTPRG(CA)	PTPRG(CA) CNTN6-Fc	406	0.98	390	17	2	284 to 579 nM
PTPRG(CA)	PTPRG(CA) CNTN6-Fc	563	0.96	332	17	2	327 to 967 nM
PTPRG(CA)	PTPRG(CA) CNTN6-Fc	579	0.96	324	17	2	344 to 975 nM
PTPRG(CA)	PTPRG(CA) CNTN6-Fc	586	0.99	254	18	1	445 to 771 nM
PTPRG(CA)	PTPRG(CA) CNTN6-Fc	465	0.97	43	17	2	315 to 686 nM
PTPRG(CA) H295A + V296A	PTPRG(CA) CNTN4-Fc	761	0.99	616	17	2	573 to 1010 nM
PTPRG(CA) H295A + V296A	PTPRG(CA) CNTN4-Fc	940	0.99	378	19	0	724 to 1220 nM
PTPRG(CA) H295A + V296A	PTPRG(CA) CNTN4-Fc	940	0.99	156	19	0	712 to 1241 nM
PTPRG(CA) H295A + V296A	PTPRG(CA) CNTN4-Fc	1028	0.97	288	19	0	686 to 1541 nM

Inhibitor	Immobilized proteins	IC_{50} (nM)	Standard deviation (nM)	n
PTPRZ(CA)	PTPRZ(CA) CNTN1-Fc	332	15	4
PTPRG(CA)	PTPRG(CA) CNTN3-Fc	428	78	7
PTPRG(CA)	PTPRG(CA) CNTN4-Fc	235	65	10
PTPRG(CA)	PTPRG(CA) CNTN5-Fc	327	39	5
PTPRG(CA)	PTPRG(CA) CNTN6-Fc	519	95	7
PTPRG(CA) H295A + V296A	PTPRG(CA) CNTN4-Fc	917	112	4

Table S2. Crystallization and freezing conditions.

Protein / Protein complexes	Conc. (μM)	Crystallization condition	Freezing solution
Human PTPRG(CA) and mouse CNTN3(Ig2-Ig3)	50	1% (v/v) Tacsimate pH 7.0, 20% (w/v) PEG 3,350, 50mM Imidazole-HCl pH 6.5	1% Tacsimate pH 7.0, 20% PEG (w/v) 3,350, 50mM Imidazole-HCl pH 6.5 and 15% (w/v) PEG 400
Mouse PTPRG(CA) and mouse CNTN6(Ig2-Ig3)	100	55% (v/v) Tacsimate pH 7.0, 150 mM NDSB 201	55% Tacsimate pH 7.0, 150 mM NDSB 201, 20% (v/v) Glycerol
Mouse CNTN5(Ig1-Ig4)	40	7% (v/v) Tacsimate pH 7.0, 15% (w/v) PEG 3,350, 50 mM Imidazole pH 7.0	50mM Imidazole pH 7.0, 5% (v/v) Tacsimate pH 7.0, 15% (w/v) PEG 3,350, 20% (v/v) Glycerol
Chicken CNTN1(FN1-FN3)	260	1% (v/v) Tacsimate pH 7.0, 20% (w/v) PEG 3,350, 50mM Imidazole pH 6.5	50 mM Imidazole pH 6.5, 9% (w/v) PEG 3,350, 21% Glycerol
Mouse CNTN2(FN1-FN3)	230	50 mM NH_4Cl, 50 mM Tris-HCl pH 8.5, 10% (w/v) PEG 4,000, 2% (v/v) glycerol	50 mM Tris-HCl pH 8.5, 10% (w/v) PEG 4,000, 25% (v/v) glycerol
Mouse CNTN3(FN1-FN3)	200	10% (w/v) PEG 1,500, 50 mM Na-cacodylate pH 6.5	25% (w/v) PEG 1,500, 50 mM Na-cacodylate pH 6.5, 10% (v/v) glycerol
Mouse CNTN4(FN1-FN3)	180	100 mM $(NH_4)_2SO_4$, 50 mM Tris-HCl pH 8.5, 10% (w/v) PEG 4,000	25 mM $(NH_4)_2SO_4$, 50 mM Tris-HCl pH 8.5, 10% (w/v) PEG 4,000, 25% (v/v) glycerol
Human CNTN5(FN1-FN3)	270	1.0 M $NH_4H_2PO_4$, 10% (v/v) Tacsimate pH 5.0	1.0 M $NH_4H_2PO_4$, 10% (v/v) Tacsimate pH 5.5, 38% (w/v) sorbitol
Mouse CNTN6(FN1-FN3)	25	300 mM Na-Malonate pH 7.0, 20% (w/v) PEG 3,350, 50 mM Na-Cacodylate pH 6.5	15% PEG 400, 20% (w/v) PEG 3,350, 250 mM Na-Malonate pH 7.0, 50 mM Na-Cacodylate pH 6.5

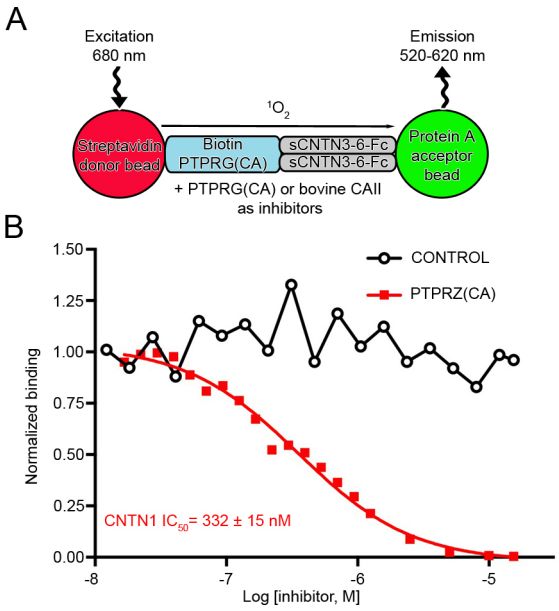

Figure S1. Interaction between the CA domain of PTPRZ with CNTN1. (A) In AlphaScreen assays, excitation of donor beads at 680 nm triggers the release of a singlet oxygen. An acceptor bead hit by this highly reactive molecule emits a signal between 520 and 620 nm. Because the half-life of the singlet oxygen is limited, a luminescent signal is only obtained when the donor beads and acceptor beads are within 200 nm. The binding of PTPRG immobilized on donor beads to Fc fusions of CNTN3-6 bound to acceptor beads brings the two beads in close proximity. Inhibition curves are obtained when increasing concentrations of an inhibitor are added to the reaction. (B) The ability of bovine CAII (control) and human PTPRZ(CA) to inhibit the AlphaScreen signal between an Fc fusion of full length mouse CNTN1 and biotin-labeled PTPRZ(CA) was assessed over a logarithmic dilution series. One representative experiment out of four is shown (Table S1).

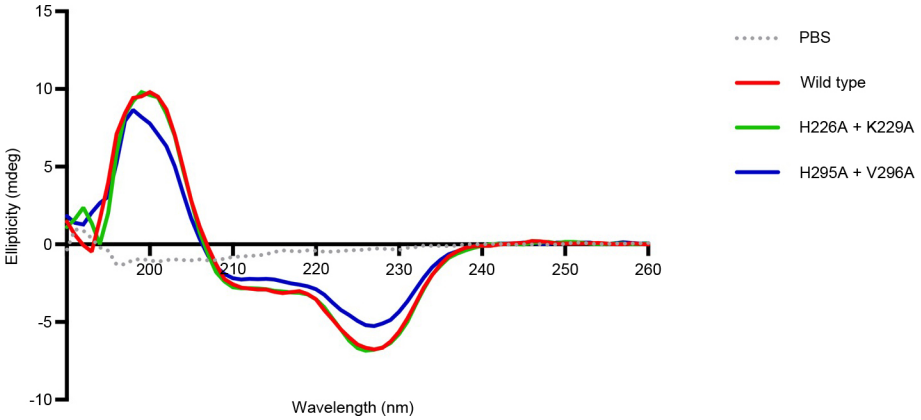

Figure S2. Circular dichroism analysis of wild type mouse PTPRG(CA) and the site directed mutants H226A + K229A and H295A + V296A. Purified mouse PTPRG(CA) and the two site-directed mutants were dialyzed extensively against phosphate-buffered saline (PBS, pH 7.4). Spectra were measured at concentrations of 0.2 mg/ml. Comparison of the three spectra indicate that the spectral features of the proteins are overall identical and the differences observed for H295A + V296A are explained by differences in the protein concentration. Overall, these experiments indicate that the mutations do not affect the secondary structure of mouse PTPRG(CA).

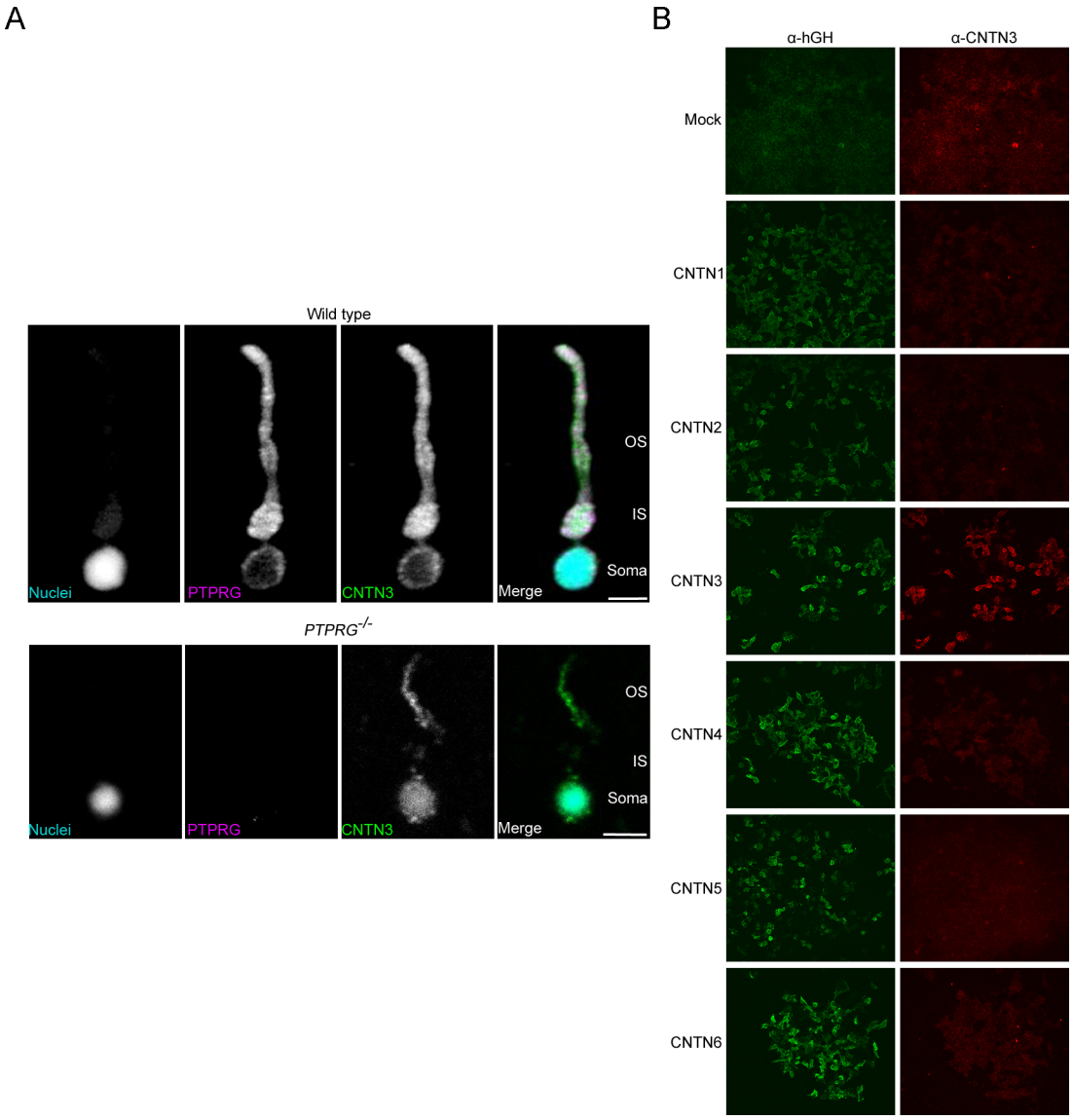

Figure S3. Validation of the PTPRG and CNTN3 antibodies. (A) The rabbit anti-PTPRG antibody used for the experiments shown in Fig. 5 stains the outer segment of an isolated mouse rod cell from a wild type mouse, but not the outer segment of a rod cell from a *PTPRG*-null mouse (1). Nuclei (blue) were visualized using RedDot™ 1 staining while PTPRG staining is shown in green. Scale bars are 5 µm. (B) Validation of the anti-CNTN3 antibody used for the experiments shown in Fig. 5. HEK293 cells transfected with full-length CNTNs fused to human growth hormone were incubated with a rabbit anti-human growth hormone antibody and with goat anti-CNTN3 antibody. The goat anti-CNTN3 recognized CNTN3 specifically.

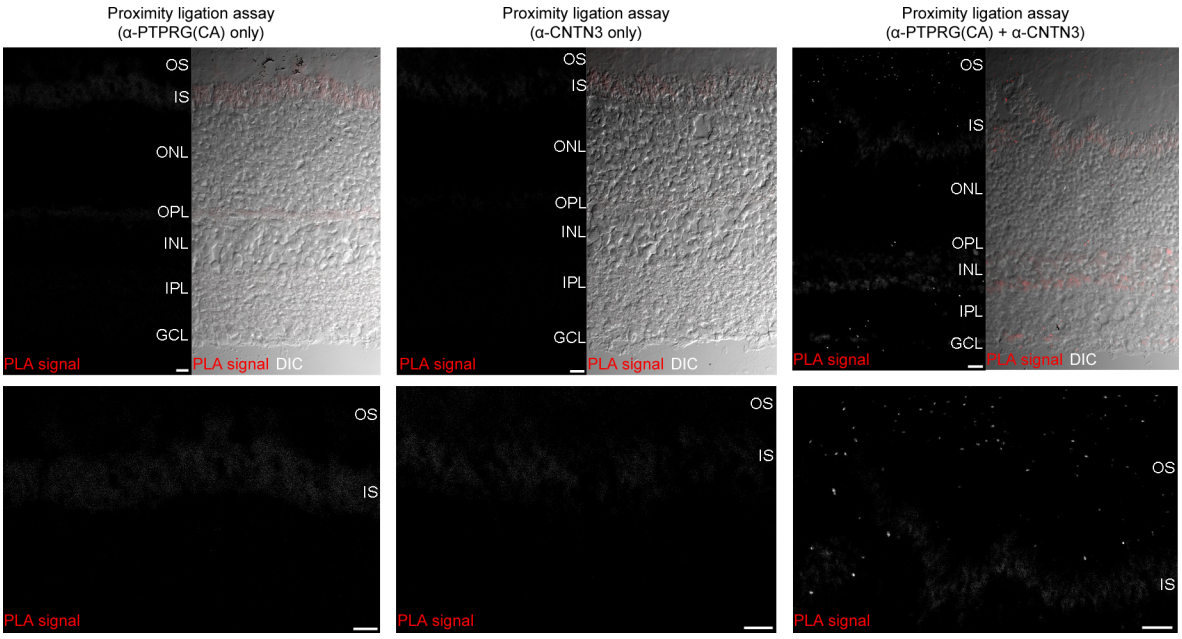

Figure S4. PTPRG and CNTN3 associate in the outer segments of mouse retinas. An *in situ* PLA shows that PTPRG and CNTN3 associate in the outer segments. This experiment includes the same goat anti-CNTN3 antibody used for the experiments shown in Fig. 5, whereas PTPRG is detected with a rabbit polyclonal antibody raised against its CA domain. Although the PLA signal is weaker than in the experiments shown in Fig. 4, comparison with the two controls strongly suggests that PTPRG and CNTN3 form a complex in the outer segments of retinas. For each experiment, a panel with PLA signal is shown next to a panel that shows the overall cellular organization of the retina in a differential interference contrast (DIC) image. A zoom of the outer segments is provided below these two panels. Scale bar is 10 µm.

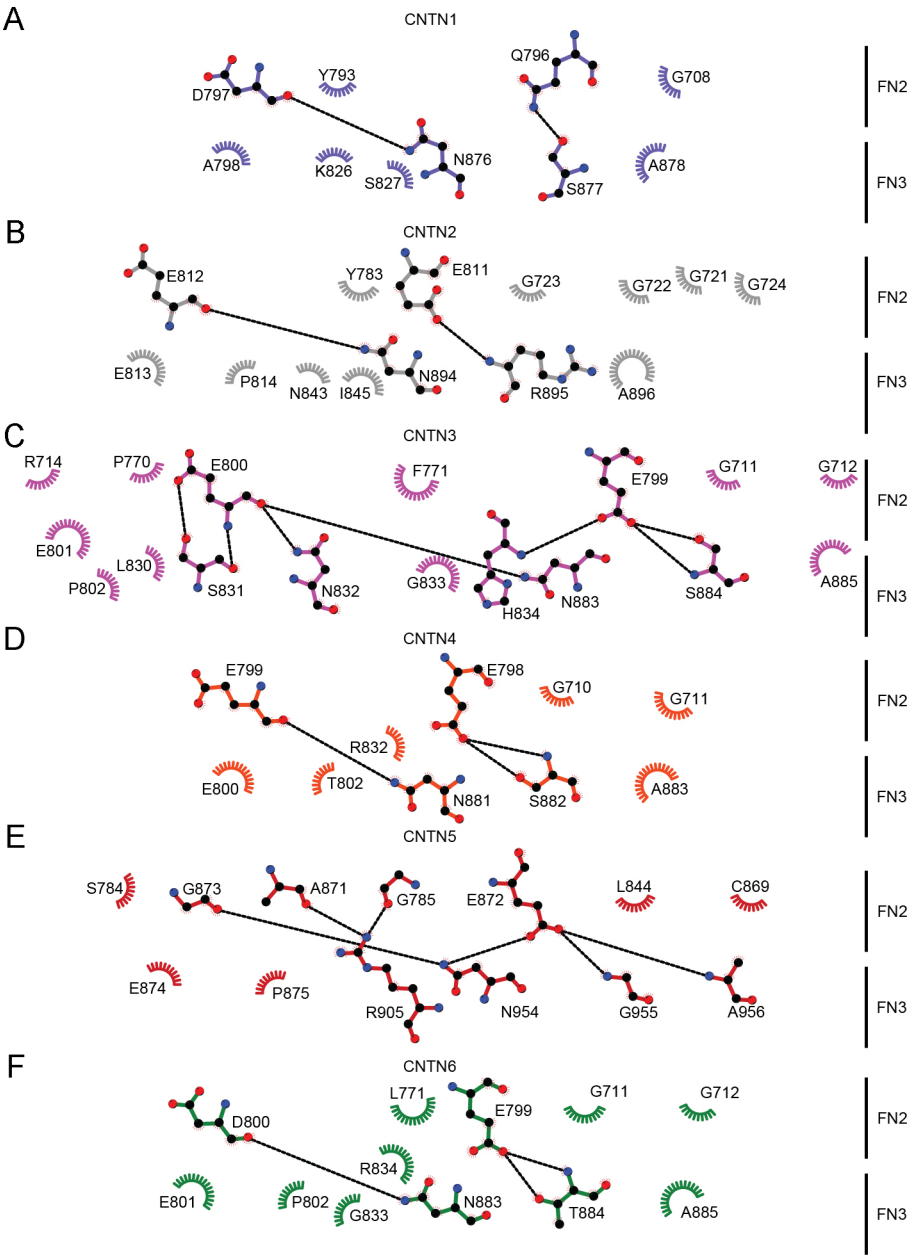

Figure S5. Conserved and specific interactions at the FN2-FN3 interfaces of CNTNs. Two-dimensional representations of the contacts at the FN2-FN3 interfaces of CNTNs were drawn using LigPlot^{+} (2). Dashed lines indicate potential hydrogen bonds while spine curves indicate residues involved in hydrophobic contacts. Although interactions mediated by the NXA residues found in a loop in FN3 are conserved in all CNTNs, most contacts at the FN2-FN3 interface are unique to each CNTN family member.

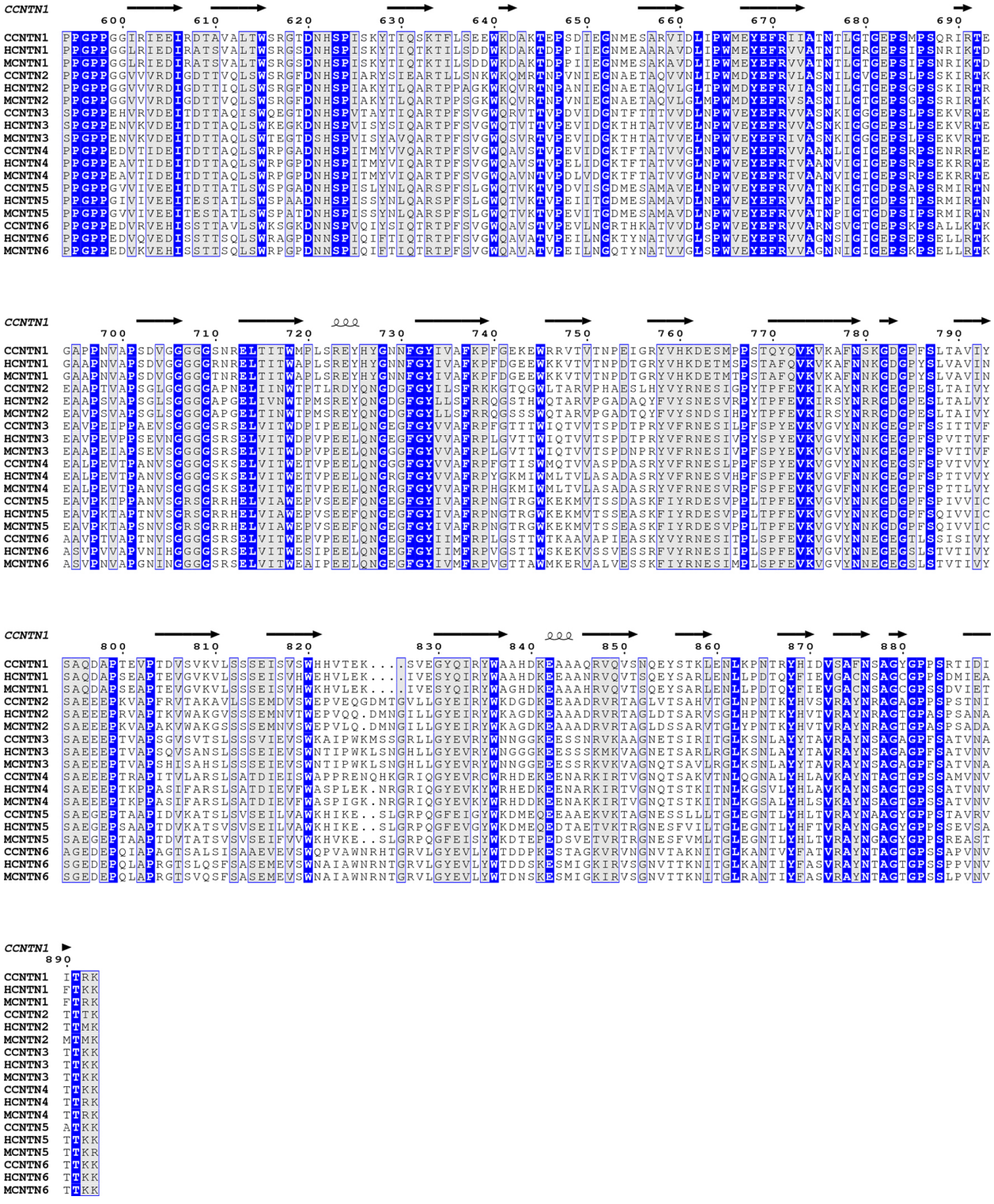

Figure S6. Alignment of amino acid sequences of domains FN1-FN3 of chicken, human, and mouse CNTN1-6. The secondary structure of chicken CNTN1 is shown above the sequence and the residue numbering corresponds to chicken CNTN1. Identical residues are shown in blue while similar residues are shaded light gray.

References

1. Lamprianou, S., Vacaresse, N., Suzuki, Y., Meziane, H., Buxbaum, J. D., Schlessinger, J., and Harroch, S. (2006) Receptor protein tyrosine phosphatase gamma is a marker for pyramidal cells and sensory neurons in the nervous system and is not necessary for normal development. *Mol Cell Biol*. **26**, 5106–5119
2. Laskowski, R. A., and Swindells, M. B. (2011) LigPlot+: Multiple Ligand–Protein Interaction Diagrams for Drug Discovery. *J. Chem. Inf. Model.* **51**, 2778–2786